Malaysian Applied Biology
https://doi.org/10.55230/mabjournal.v55i3.3917

Research Article

Anti-HHV-1 Mechanism and Pharmacokinetic Profile of Bioactive Compounds from *Phaleria macrocarpa* (Scheff.) Boerl Fruit

Nazlina Ibrahim[1]*, Poomangalaththazha Kuniyil Safariya[1], Anis Sofea Azman[1], Khairul Azreena Bakar[1,2], Su Datt Lam[3] & Mahmud Y. Y. Ismaeel[1,4]

[1]*Department of Biological Sciences and Biotechnology, Faculty of Science and Technology, Universiti Kebangsaan Malaysia, Bangi 43600, Selangor, Malaysia.*
[2]*Department of Medical Microbiology and Parasitology, School of Medical Sciences, Universiti Sains Malaysia, Kubang Kerian 16150, Kelantan, Malaysia.*
[3]*Department of Physics, Faculty of Science and Technology, Universiti Kebangsaan Malaysia, Bangi 43600, Selangor, Malaysia.*
[4]*Department of Medical Science, Abbs Community College, Hajjah, Yemen.*

**Corresponding author: nazlina@ukm.edu.my*

ABSTRACT

This study reports on *Phaleria macrocarpa* fruit protein aqueous extract (PMFPAE) compounds, the mechanistic anti-human herpes virus type-1 (HHV-1) insights, and pharmacokinetic profiles. The mechanistic insight of PMFPAE treatment on the virus *UL27* gene expression that encodes the viral attachment glycoprotein, gB, was determined to be downregulated at all replication phases, especially at 8 hr post-treatment, concurring with the late replication phase. Seven main water-soluble compounds in PMFPAE were identified via liquid chromatography-tandem mass spectrometry (LC-MS/MS). These include organic acids (D-gluconic acid), xanthones (mangiferin, homomangiferin), and flavonoids (quercetin, myricetin 5-methyl ether, oroxylin A, and apigenin 7-glucuronide-4′-(6′′-malonylglucoside)). All the compounds have drug-likeness properties according to Lipinski's Rule of Five except for apigenin 7-glucuronide-4′-(6′′-malonylglucoside). Except for quercetin and oroxylin A, the compounds have low gastrointestinal absorption, indicating low possibility for oral use. ProTox-II predicted D-Gluconic acid as the least toxic, and quercetin has the highest toxicity. CarcinoPredEL indicated none of the compounds to be carcinogenic. In molecular docking studies, two compounds, homomangiferin and apigenin 7-glucuronide-4'-(6'' malonylglucoside), showed strong binding affinity towards virus glycoprotein gB. Five compounds have strong binding towards the virus glycoprotein gD, including mangiferin, myricetin 5-methyl ether, homomangiferin, apigenin 7-glucuronide-4'-(6'' malonylglucoside), and quercetin. Homomangiferin can bind to both virus attachment glycoproteins gB and gD, with additional antioxidant and anti-inflammatory activities. Strong binding affinities of mangiferin and homomangiferin to site I (subdomain IIA) of human serum albumin (HSA) suggest effective compound transport within the bloodstream, enhancing their stability and half-life. In conclusion, PMFPAE consists of multifacet drug-like bioactive compounds that inhibit viral entry by binding to gB and gD and have antioxidant and anti-inflammatory activities. The predicted pharmacokinetic profile suggests that compounds of PMFPAE are more suitable for development as an anti-HHV topical agent due to the limited gastrointestinal absorption, toxicity of several key compounds, and limited binding to HSA.

Key words: Anti-human herpes virus Type-1 (HHV-1) activity, mechanism, in silico, *Phaleria macrocarpa* (mahkota dewa), pharmacokinetic, bioactive compounds

Article History

Accepted: 13 July 2026
First version online: 30 August 2026

Cite This Article:
Ibrahim, N., Safariya, P.K., Azman, A.S., Bakar, K.A., Lam, S.D. & Ismaeel, M.Y.Y. 2026. Anti-HHV-1 mechanism and pharmacokinetic profile of bioactive compounds from *Phaleria macrocarpa* (Scheff.) Boerl fruit. Malaysian Applied Biology, 55(3): 1-14. https://doi.org/10.55230/mabjournal.v55i3.3917

INTRODUCTION

Human Herpesvirus Type 1 (HHV-1) is a highly infectious pathogen primarily transmitted through direct contact with infected secretions (Laine *et al.*, 2015). The most common HHV-1 clinical manifestation is oral mucocutaneous lesions, but it can lead to severe clinical complications, including keratitis, neonatal infections, and life-threatening encephalitis—particularly in immunocompromised individuals (Azher *et al.*, 2017; Crimi *et al.*, 2019; Dähne *et al.*, 2025). HHV-1 is the leading cause of infectious blindness and can trigger Eczema Herpeticum in children with potentially fatal complications of atopic dermatitis if not treated (Farooq & Shukla, 2012; Bin *et al.*, 2014).

Acyclovir (ACV) remains the gold-standard, first-line treatment for both primary and recurrent HHV-1 infections due to its high specificity in inhibiting viral DNA replication (Gnann *et al.*, 1983). However, the prolonged and often unregulated use of ACV—partic-

ularly for long-term prophylaxis—has spurred the emergence of resistant viral strains (Piret & Boivin, 2011; Wang *et al.*, 2011). This rising resistance underscores an urgent need for novel antiviral agents with distinct mechanisms of action able to bypass the current clinical challenges.

Natural products offer a promising reservoir for such therapeutic agents. *Phaleria macrocarpa* (Scheff.) Boerl., commonly known as Mahkota Dewa, is traditionally utilised in health supplements and cosmetics to treat various ailments, including diabetes, hypertension, and cancer (Kalusalingam *et al.*, 2024). The plant's therapeutic potential is attributed to a rich profile of secondary metabolites, such as flavonoids, terpenoids, and phenolic compounds (Ismaeel *et al.*, 2015, 2018a, 2018b). While these metabolites have been identified in various other extracts, the specific chemical composition of the *P. macrocarpa* fruit protein aqueous extract (PMFPAE) remains unreported. Characterising these bioactive compounds is essential for providing information on the pharmacological characteristics of the active compounds. A previous study has demonstrated that PMFPAE possesses virucidal activity and inhibits both viral entry and progeny release (Ismaeel *et al.*, 2024). Furthermore, it effectively interferes with the early and late replication phases of the viral life cycle (Ismaeel *et al.*, 2022). Another aspect that needs to be confirmed is the inhibitory effect of PMFPAE on the expression of the UL27 gene encoding the virus surface glycoprotein B, gB. This will provide complementary evidence on the impact of PMFPAE on HHV-1 replication since gB is the mandatory glycoprotein release of capsid into the host cytoplasm (Cattaneo *et al.*, 2025). Downregulation of *UL27* can explain why the physical fusion of the virus into the host collapses.

Developing PMFPAE-based therapeutics or supplements needs information regarding the "oral drug-likeness", toxicity, carcinogenicity, bioavailability, rapid systemic clearance, and distribution in the body (Ezike *et al.*, 2023). Human Serum Albumin (HSA), the primary carrier protein in plasma, plays a pivotal role in pharmacokinetics. While HSA can extend the circulatory half-life of a drug, excessively high binding affinity may reduce the concentration of the "free" active drug available at the site of infection (Tayyab & Feroz, 2021). Consequently, understanding the binding dynamics between PMFPAE components and HSA is vital for predicting their therapeutic potential.

Thus, this study aims to bridge these knowledge gaps on the effect of PMFPAE on the UL27 gene expression that encodes HHV-1 gB by integrating LC-MS/MS profiling with in silico ADME predictions and molecular docking to explore the molecular interactions governing the antiviral properties, pharmacokinetics, toxicity, and delivery of PMFPAE to the site of HHV-1 infection. We hypothesized that bioactive compounds present in PMFPAE contribute to anti-HHV-1 activity through modulation of viral glycoproteins and possess favourable pharmacokinetic characteristics.

MATERIALS AND METHODS

Plant extract preparation

The extract known as PMFPAE was prepared following the methodology described by Ismaeel *et al.* (2022).

Gene expression analysis

Vero cells were grown in 25 cm² cell culture flasks (SPL Life Sciences, Korea) to reach 80% confluence. Cells were infected with the HHV-1 clinical strain at 0.05 MOI for 2 hr, and then the virus inoculum was removed. Cells were treated with PMFPAE at 60 µg/mL for 4, 8, 12, or 24 HPI. Viral RNA was isolated at the different time points using the TRIsure^{TM} kit (Bioline) and subjected to reverse transcription to produce cDNA using the Tertro cDNA synthesis kit (Bioline). The primer sequences for U_L27 and the reference gene (*RPL32*), and the annealing temperature are listed in Table 1. The RPL32 gene served as the housekeeping gene (HKG) and internal reference to normalize the quantity of mRNA within the samples in qRT-PCR (Iberahim *et al.*, 2018). Results were expressed as the mean ± standard deviation (SD). The experiments were performed in triplicate, with the mean values representing three experiments. Statistical data analysis was conducted using one-way ANOVA by SPSS (p<0.05 considered significant).

In the qRT-PCR analysis, the reagent mix for each reaction includes: 0.8 µL of each primer [(10 µM, forward & reverse), total volume 1.6 µL], 7.4 µL of nuclease-free water (NFW), and 10 µL of the (2× SaniFast SYBR & Fluorescein Mix Kit, Bioline, USA). Reagent mix (19 µL) was dispensed into a 96-well PCR plate, and 1 µL of cDNA sample (50 ng) was added to the designated well and thoroughly mixed. The plate was securely sealed with an adhesive membrane and then centrifuged for 30 sec at 234 ×g. Quantitative PCR (qPCR) was conducted using a real-time PCR machine (Bio-Rad iQ5, Invitrogen Life Science Technologies, USA) under the following conditions: activation of the polymerase enzyme at 95℃ for 10 min, subsequent annealing process at 95℃ for 15 sec for 40 cycles, and elongation at 60℃ for 1 min. The melting curve of qPCR reactions was analyzed for both the target and the reference genes using the default instrument settings. Data analysis was done using relative gene expression ($2^{-\Delta\Delta Ct}$) (Livak & Schmittgen, 2001).

Identification of PMFPAE compounds by LC-MS/MS

PMFPAE was separated using a C18 column (Acclaim^{TM} Polar Advantage II, 3 × 150 mm, 3 µm particle size, Thermo Scientific) on a Dionex UltiMate 3000 ultra-high performance liquid chromatography (UHPLC) system, and high-resolution mass spectrometry (MS) was achieved using a Bruker Daltonics micrOTOF-Q III. The system was operated with electrospray ionization (ESI) in negative ionization mode (Hua & Jenke, 2012). The capillary voltage was set to 4000 V, the nebulizer pressure was set to 2.0 bar, and the drying gas was set to 8 L/min at 300℃. Gradient elution was performed using A: 0.1% formic acid in Milli-Q water, pH 3.2, and B: 100% acetonitrile (ACN) at a flow rate of 0.2 mL/min and column temperature of 40℃. PMFPAE was injected in a 1 µL volume, and the test was carried out using a gradient elution technique with a total run time of 22 min. The gradient began at 5% B (0-3 min), then increased to 80% B (3-10 min), 80% B (10-15 min), and lastly 5% B (15-22 min). For compound identification, the peak mass spectra were compared to data from the literature and library (Horai *et al.*, 2010). The MS range (m/z) was between 50 and 1000 Da.

Ligand selection and preparation

The 2D structures of the compounds reported from the LC-MS/MS analysis were obtained from the PubChem database. The structures

Table 1. Primer sequences of target and reference genes, and annealing temperature for qRT-PCR reaction (Iberahim *et al.*, 2018).

Genes	Forward and Reverse primer sequence	Annealing temperature (°C)
U_L27	F (5′-ACGGGACGACGGTAAACTGC-3′) R (5′-TGGTGTGTTCGGTGTGCGAC-3′)	58.2
RPL32	F (5′-AACATTCCATCTCCTCCTCGG-3′) R (5′-TTGACATACCGGTCTGACTGGTGC-3′)	55

underwent a purification and optimization process using AutoDock Tools 1.5.6. This preparation involved converting the 2D structures into three-dimensional (3D) structures and energy minimization using Avogadro. This was followed by the assignment of appropriate Gasteiger/Kollman charges and merging non-polar hydrogens to ensure the ligands were in a stable, energetically favourable state for subsequent docking simulations (Pattanaik & Bhadra, 2020). To identify the binding locations of the compounds on HSA, the 3D structures of the seven compounds were converted to PDBQT format using OpenBabel 3.1.1 and optimized for geometry in Chem3D.

Target protein identification and active sites

a) HHV-1 target proteins

HHV-1 target proteins and their active sites were identified according to Pattanaik & Bhadra (2020). These proteins were selected based on a resolution of less than 3.0 Å, ensuring high structural quality, a well-defined molecular arrangement, and precise atom visibility. To maintain the integrity of the final protein conformation and ensure no unintended bias in the simulation, only wild-type structures free from mutations or synthetic modifications were utilised. Target proteins that were identified include glycoprotein B (gB) and glycoprotein D (gD) as the key surface proteins involved in viral attachment to host cells. The crystal structures of gB (PDB ID: 3NWF) and gD (PDB ID: 4MYV) were retrieved from the RCSB Protein Data Bank. Structural reliability was further validated by a Ramachandran outlier percentage of less than 0.5% and an R-factor value of below 0.5, which are benchmark indicators of a high-quality model suitable for docking studies. Models exceeding these thresholds were excluded to avoid inaccuracies stemming from poor backbone geometry. The selected PDB structures—which contained crystallographic water molecules, heavy atoms, cofactors, and metal ions—were imported into Discovery Studio 2021 for systematic purification. Protein refinement involving the removal of all non-essential molecules, including ligands and heteroatoms, was performed using UCSF ChimeraX. To complete the structural valency, hydrogen atoms were added, and Kollman charges were assigned to stabilize the electrostatic potential of the protein environment (Pattanaik & Bhadra, 2020).

b) Human serum albumin

The high-resolution structure of HSA (PDB ID: 1BM0) was used, and docking simulations were set up where the ligands were flexible and the protein was rigid. The ligands' rotatable bonds were defined by merging nonpolar hydrogens, and polar hydrogens were added to the protein while removing water and non-relevant ligands.

Molecular docking protocol

a) The docking procedure between HHV-1 proteins and compounds, or identification of the binding locations of the compounds to HSA, was adapted from Huey and Morris (2008). The active site coordinates were defined based on the binding pocket predictions obtained from the PrankWeb server. Initial virtual screening to determine binding affinities was conducted using AutoDockTools v.1.2.7 and AutoDock 4.26 tools and followed by docking simulations using PyRx, 0.8. Compounds exhibiting the highest binding affinity values towards the target proteins were subsequently selected for more rigorous and detailed docking analysis.

Post-docking visualization and interaction analysis

a) Molecular docking was employed to predict the optimal binding conformations between the target proteins and the identified compounds that act as the ligands. The resulting docking complexes were visualized and analysed using Discovery Studio 2021. The output files were imported into the software to map the active site architecture and ligand orientation.

Key docking parameters evaluated included the types of intermolecular interactions, the specific amino acid residues involved, and the bond distances (Å) between the residues and the ligands (Hernández-Santoyo *et al.*, 2013). Two-dimensional (2D) interaction diagrams were generated to characterize the binding forces, including hydrogen bonding, Van der Waals forces, Pi-cation, Pi-anion, Pi-alkyl, Pi-sulfur, Pi-sigma, and Pi-donor hydrogen bonds, as well as any unfavourable interactions. The docking results were then visualized in 3D using PyMOL software to look for binding positions of protein and compounds as ligands.

b) For compound-HSA docking, 100 independent runs were performed at two key binding sites in subdomains IIA and IIIA of HSA, with specific grid box dimensions and centers defined for each site based on a previous study (Bakar *et al.*, 2024). The binding energy was calculated using the Lamarckian genetic algorithm. The best conformations with the lowest binding energy were selected for analysis, and ligand-protein interactions were visualized using AutoDockTools and UCSF Chimera. Additionally, Biovia Discovery Studio was utilized to predict the intermolecular forces contributing to these interactions.

Pharmacokinetics prediction

The prediction was conducted to evaluate the drug-likeness, physicochemical characteristics, and pharmacokinetic profiles—including absorption, distribution, metabolism, and excretion (ADME) properties—of the bioactive compounds, analysed using the SwissADME web server (Daina *et al.*, 2017). The Canonical SMILES (Simplified Molecular Input Line Entry System) strings for the compounds were retrieved from the PubChem database and processed through the SwissADME platform.

Toxicity prediction

Toxicity prediction of compounds was performed to determine and verify that the drug was safe for human use. The analysis was performed using ProTox-II (February 2021 version). ProTox-II is a web server for the in silico prediction of oral toxicities of compounds (Banerjee *et al.*, 2018). The 2D structure of the compounds was uploaded to the server, which yielded results revealing the toxicity prediction.

Carcinogenicity prediction

Carcinogenicity prediction of compounds was performed using the CarcinoPred-EL (Carcinogenicity Prediction using Ensemble Learning Methods) online webserver. This webserver helps to classify compounds as carcinogens and non-carcinogens using their 2D structures. The 2D structures of compounds were drawn at the interface of the CarcinoPred-EL website. The CarcinoPred-EL webserver was run, and the output result was generated.

RESULTS AND DISCUSSION

PMFPAE reduces UL27 expression at all replication phases

Figure 1 illustrates the expression levels of U_L27 genes at different time points in HHV-1 following treatment with PMFPAE. The designated time points represent virus replication phases, specifically at 4 HPI (early replication), 8 HPI (mid-replication), 12 HPI (late phase), and 24 HPI, which is the progeny reinfection as previously indicated by Ismaeel *et al.* (2022). The U_L27 gene that encodes gB, the envelope surface on the virion, showed down-regulation, indicating PMFPAE's influence on this gene during all phases of HHV-1 replication, with the highest inhibition of almost a two-fold change during the mid-replication phase at 8 HPI. A previous study by Ismaeel *et al.* (2022) noted that PMFPAE plaque inhibition percentage towards the HHV-1 clinical strain was about 85% at 2 HPI and around 70% inhibition at 4 HPI, which correlates with one-fold inhibition of the U_L27 gene. At 8 HPI, plaque inhibition is around 50% and almost 2-log-fold of U_L27 gene inhibition. Prolonged treatment with PMFPAE up to 24 hr can be considered as the reinfection of progeny with 80% plaque inhibition in a time-of-removal study, and from this study, ½-fold of U_L27 gene inhibition.

Table 2. List of peak compounds identified in PMFPAE by LC-MS/MS analysis with their reported biological activities.

Compound / Molecular formula / Class	R_t (min)	$[M-H]^-$ (m/z)	MW (g/mol)	MS^2 (m/z)	Biological activity
D-Gluconic acid $C_6H_{12}O_7$ Organic acid	2.1	195.051	196.16	129.0201 (291), 194.9044 (103), 195.0519 (268)	Inhibits viral replication by inhibiting virus attachment or penetration (Santoyo *et al.*, 2012)
Mangiferin $C_{19}H_{18}O_{11}$ Xanthone	8.5	421.08	422.33	–*	Antioxidant (Khurana *et al.*, 2016); virucidal activity (Du *et al.*, 2018; Rechenchoski *et al.*, 2020); targeted inhibitor of the UL54 gene (Kim *et al.*, 2021; Wang & Chen, 2023)
Myricetin 5-methyl ether $C_{16}H_{12}O_8$ Flavonoid	8.5	331.047	332.26	259.0263, 271.0260, 272.0328, 301.0371, 302.0405, 313.0376, 331.0377, 332.0514, 373.0586, 391.0693	Direct interaction with the virus gD protein and cellular EGFR/PI3K/Akt pathway related to cell cycle (Li *et al.*, 2020)
Homomangiferin $C_{20}H_{20}O_{11}$ Xanthone	9.2	435.09	436.40	–*	Antioxidant (Masibo & He, 2008; Andrean *et al.*, 2014; Lay *et al.*, 2014); disrupts HHV-1 by interacting with the gD entry process, effectively "blocking" the gB glycoprotein (Fan *et al.*, 2015)
Apigenin 7-glucuronide-4′-(6′′-malonylglucoside) $C_{30}H_{30}O_{19}$ Flavonoid	10.0	693.10	694.50	259.0636, 301.0371, 313.0388, 331.0478, 343.0509, 421.0808, 422.0843, 433.0808, 434.0825, 693.1353	Reduces viral progeny production (Qiu *et al.*, 2019; Salehi *et al.*, 2019)
Quercetin $C_{15}H_{10}O_7$ Flavonoid	11.4	301.03	302.24	116.9275, 301.0359, 302.0389, 343.0468, 355.0462, 356.0512, 373.0579, 374.0616, 521.1091, 522.1133	Blocks the early stage of virus replication/viral entry and shows diverse antiviral modes of action (Chiang *et al.*, 2003; Saakre *et al.*, 2021; Lee *et al.*, 2017; Biancatelli *et al.*, 2020) and anti-inflammatory activity (Ruiz *et al.*, 2007; Martínez-Flórez *et al.*, 2005)
Oroxylin A $C_{16}H_{12}O_5$ Flavonoid	13.1	283.0612	284.26	–*	Anti-inflammatory (Lee & Park, 2016)

R_t: retention time; MW: molecular weight; *m/z*: mass-to-charge ratio; MS^2: fragments for the related molecular ions. *MS2 spectra were not acquired for mangiferin, oroxylin A, and homomangiferin due to intensities failing to meet the Data-Dependent Acquisition (DDA) trigger threshold. Identification for these peaks was confirmed via high-resolution MS1 data (<5 ppm mass error) and isotopic pattern matching (mSigma values).

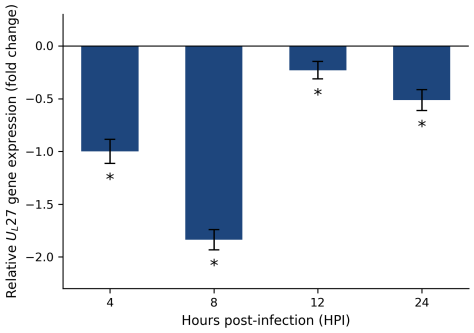

Fig. 1. Calculated relative *UL27* gene expression levels in PMFPAE-treated virus relative to the expression levels of untreated virus. U_L27 gene expression levels in the HHV-1 clinical strain at different time points of 4, 8, 12, and 24 HPI are all down-regulated, indicating PMFPAE's influence on this gene during all phases of HHV-1 replication, with the highest inhibition of almost a two-fold change during the mid-replication phase at 8 HPI. *Indicates significant difference compared to lower gene expression in PMFPAE-treated virus (p<0.05). The values represent mean ± SD (n=3).

Compounds in PMFPAE

The LC-MS/MS chromatogram in Figure 2 revealed a range of diverse compounds with seven distinct peaks, with the highest to

lowest concentration as follows: mangiferin > myricetin 5-methyl ether > oroxylin A > homomangiferin > apigenin > D-gluconic acid > quercetin. The compound class, retention time, molecular weight, mass-to-charge ratio (m/z), molecular formula, and reported biological activity, including antiviral potential, are listed in Table 2.

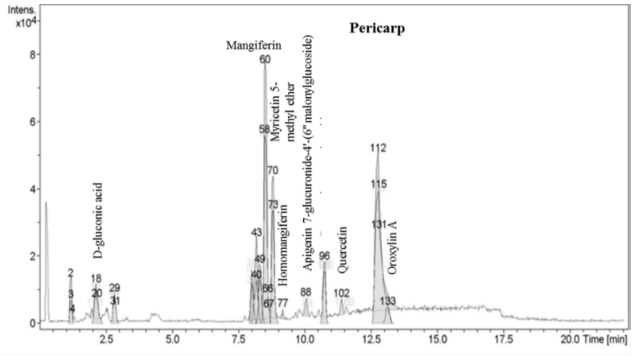

Fig. 2. LC/MS-MS chromatogram of PMFPAE in negative ionization mode. Table 2 provides information on seven compounds with the highest peaks.

Compounds' predicted drug-likeness, physiochemical properties and pharmacokinetic

To be an effective drug, a compound must be characterized by optimal solubility in both water and fat. Lipophilicity determines biological processes and is related to the absorption, bioavailability, hydrophobic drug-receptor interactions, metabolism, and toxicity. The calculated logarithm of the octanol/water partition coefficient, also known as log $P_{o/w}$, is used to estimate solubility (Lipinski *et al.*, 2001; Kovačević *et al.*, 2014). For the compounds to be categorised as drug-like molecules, they have to meet at least 2 rules out of the five Lipinski's rules (Lipinski *et al.*, 2001). Table 3 shows data for drug-likeness of all the compounds; quercetin, mangiferin and myricetin 5-methyl ether have the least Lipinski's rule violations, hence can be considered as drug-like molecules.

According to Veber's Rule (Veber *et al.*, 2002), a compound is predicted to have good oral bioavailability if it meets two primary criteria, which emphasize molecular flexibility and polar character. To satisfy Veber's criteria, a molecule must have 10 or fewer rotatable bonds (RB) and a Total Polar Surface Area (TPSA) of ≤ 140 Å². Alternatively, the rule suggests that a compound may also be considered drug-like if it has a total count of hydrogen bond donors and acceptors of 12 or fewer. In this study, all compounds except apigenin can be considered to be drug-like molecules with consideration to be absorbed by the gastrointestinal (GI) tract and maintain their efficacy, as they met 2 out of the five rules. Quercetin and oroxylin A have high GI absorption, but other compounds have low GI absorption. Further evaluation of the *in vivo* antiviral properties will allow suggestions on the use of PMFPAE for oral or perhaps topical use.

D-Gluconic Acid, Quercetin and Oroxylin A pass Veber Rule Compliance. Mangiferin, Myricetin, Homomangiferin and Apigenin 7-glucuronide-4′-(6′′-malonylglucoside) fail Veber's Rule Compliance. In drug discovery, compounds with high PSA, like Mangiferin and Myricetin, suggest poor membrane permeability, which means that while these compounds might inhibit CYP enzymes in a test tube (*in vitro*), they may not reach high enough concentrations in the liver (*in vivo*) to cause significant drug-drug interactions.

Quercetin is well-known for its ability to interfere with drug metabolism. It adheres to Veber's rules, suggesting good oral absorption, which increases the risk of it reaching the liver and inhibiting

Table 3. Drug-likeness prediction using Lipinski's Rule of Five and Veber's Rule.

Compound ID	MW (g/mol)	Log P	MR (cm³/mol)	HBD	HBA	Lipinski (of 5)	RB	TPSA (Å²)	GI Absorption	CYP450 inhibition
D-Gluconic Acid, $C_6H_{12}O_7$	196.16	−2.42	40.40–41.50	6	7	4/5	5	138.45	Low	Generally non-inhibitory; primary metabolic fuel
Mangiferin, $C_{19}H_{18}O_{11}$	422.34	−0.77	97.10–98.50	8	11	3/5	2	201.28	Low	Weak inhibitor of CYP3A4 and CYP2C9
Myricetin, $C_{16}H_{12}O_8$	332.26	0.98	77.10–78.40	5	8	5/5	2	140.59	Low	Potent inhibitor of CYP2C9 and CYP3A4
Homomangiferin, $C_{20}H_{20}O_{11}$	436.37	−2.32	101.80–103.20	7	11	4/5	3	190.28	Low	Similar to Mangiferin; low metabolic interference
Apigenin 7-glucuronide-4′-(6′′-malonylglucoside), $C_{30}H_{30}O_{19}$	694.55	−1.92	151.00–156.00	9	19	1/5	11	309.64	Low	Highly polar; unlikely to reach hepatic CYPs easily
Quercetin, $C_{15}H_{10}O_7$	302.24	1.23	75.10–76.60	5	7	5/5	1	131.36	High	Competitive inhibitor of CYP2C19, CYP3A4, and CYP2D6
Oroxylin A, $C_{16}H_{12}O_5$	284.26	2.56	76.40–77.90	2	5	5/5	2	79.90	High	Moderate inhibitor of CYP1A2 and CYP3A4

MW ≤ 500; Log P < 5; MR between 40–130; HBD ≤ 5; HBA ≤ 10; RB ≤ 10; TPSA ≤ 140 Å².

Table 4. Drug parameters and toxicity report of compounds.

Compound	Molecular weight (g/mol)	Molar Refractivity	Predicted LD_{50} (mg/kg)	Toxicity class	Status
D-Gluconic acid	196.18	38.54	9100	6	Non-Toxic
Mangiferin	302.24	78.04	159	3	Toxic
Myricetin 5-methyl ether	332.26	84.53	5000	5	May be harmful
Homomangiferin	436.07	105.17	562	4	Harmful
Apigenin 7-glucuronide-4′-(6′′-malonylglucoside)	694.55	155.16	500	5	May be harmful
Quercetin	422.34	100.7	2	1	Fatal
Oroxylin A	284.26	78.46	4000	5	May be harmful

Table 5. Carcinogenicity prediction of compounds with predicted probabilities >0.8.

Compound ID	RF (Avg)	SVM (Avg)	XGBoost (Avg)	Consensus Probability	Prediction Class
Apigenin	0.40	0.39	0.44	0.41	Non-Carcinogen
D-Gluconic acid	0.15	0.18	0.39	0.40	Non-Carcinogen
Homomangiferin	0.39	0.49	0.07	0.24	Non-Carcinogen
Mangiferin	0.37	0.43	0.07	0.33	Non-Carcinogen
Myricetin	0.64	0.83	0.07	0.44	Non-Carcinogen
Oroxylin A	0.73	0.79	0.07	0.46	Non-Carcinogen
Quercetin	0.62	0.71	0.07	0.41	Non-Carcinogen

CYP3A4 (the enzyme responsible for metabolising approximately 50% of all drugs).

Myricetin has been shown in studies to significantly inhibit CYP2C9 activity, which can affect the metabolism of drugs like warfarin or ibuprofen. Apigenin 7-glucuronide-4′-(6′′-malonylglucoside) is a large, highly decorated flavonoid glycoside and a "Veber outlier." In its intact form, it is too polar to pass through cell membranes effectively. It acts as a "pro-drug" in the gut, where bacteria must first strip away the sugars before the aglycone (Apigenin) can be absorbed and potentially interact with CYP enzymes.

Toxicity prediction and compounds characteristic

Compounds that act as a ligand were subjected to toxicity prediction, tabulated in Table 4. There are six classes for toxicity (1-6) in ProTox-II, with class 1 having LD_{50} ≤5, indicative of toxicity that can lead to fatality, while class 6 has LD_{50} >5000, indicating non-toxicity (Banerjee *et al.*, 2018). ProTox-II prediction revealed that D-Gluconic acid (Class 6) was the least toxic, followed by Myricetin 5-methyl ether, Oroxylin A, and the Apigenin derivative (Class 5), while Quercetin (Class 1) and Mangiferin (Class 3) exhibited the highest toxicity. From a pharmacological perspective, Homomangiferin and the Apigenin derivative are the strongest candidates to be considered as drugs because they combine high safety profiles with exceptional binding affinities against viral proteins. Therefore, while several compounds show promise, Homomangiferin stands out as the most viable lead due to its balance of potent inhibitory activity and a manageable toxicity rating.

Carcinogenicity prediction

The carcinogenicity of the seven selected ligands from *Phaleria macrocarpa* was evaluated using an ensemble learning approach (RF, SVM & XGBoost), which confirmed that all compounds are classified as Non-Carcinogens. With consensus probabilities ranging from 0.24 to 0.46, all scores fall well below the 0.50 threshold, indicating a lack of DNA-damaging or cancer-promoting properties. Homomangiferin yielded the lowest risk score (0.24), reinforcing its status as a top lead candidate, while D-Gluconic acid served as a reliable non-toxic benchmark at 0.40. Despite minor variations in the XGBoost model for certain flavonoids, the overall internal consistency across all models suggests that these natural polyphenolic structures are recognised as safe metabolites. Ultimately, this *in silico* screening provides vital evidence that these compounds, particularly Homomangiferin, are safe for further *in vitro* and *in vivo* testing without the risk of chemical-induced malignancy.

Compound-virus protein interaction

a) Virus proteins active sites

The molecular docking study is focused on two glycoproteins, namely gB and gD, in relation to previous reports on antiviral activity affecting virucidal activity, early and late replication phases, and finally virion release (Ismaeel *et al.*, 2022; Ismaeel *et al.*, 2024). The results in UL27 gene expression above make it more logical to focus on the surface proteins, namely the glycoproteins gB and gD. Validation of the structural reliability was done and shown in Table 6. Although the Ramachandran plot for glycoprotein D indicated that >0.5% of residues were in the outlier region, the structure was deemed acceptable for molecular docking. This decision was based on the fact that the identified outliers were located outside the predicted binding pockets and did not interfere with the overall structural integrity or the active sites' geometry required for the simulation.

b) Compound-virus target protein interactions

The compounds' binding affinities and specificity of interactions with virus proteins gB or gD following molecular docking are tabulated in Table 7 and illustrated in Figures 3 and 4. Binding affinity is defined as the change in free energy associated with the binding process, where the magnitude of this affinity indicates the strength of the interaction between a protein and a ligand (Wan *et al.*, 2020). Consequently, a high binding affinity value confirms a strong and stable interaction between the two structures, suggesting a highly focused interaction compared to other potential ligands.

Table 6. Resolution value, Ramachandran percentage, R value and mutation for HHV-1 active proteins.

Protein Name (PDB ID)	Resolution Value (<3.0 Å)	Ramachandran Outliers (%)	Factor R Value (<0.5)	Mutation	Reference
Glycoprotein B (3NWF)	3.00 Å	0.4%	0.249	None	Stampfer *et al.*, 2010
Glycoprotein D (4MYV)	1.80 Å	0.6%	0.230	None	Li *et al.*, 2020

Table 7. Binding affinity of ligands (compounds) to glycoproteins gB and gD, hydrogen bond interaction, hydrophobicity interaction, and interpretation.

Ligand / Target	Binding Affinity (kcal/mol)	Key Hydrogen Bond Interactions	Key Hydrophobic Interactions	Interpretation
D-Gluconic acid / 3NWF (gB)	−5.4	ASN548, ALA561, GLU622, THR626, LEU625, CYS116	–	Weak interaction with limited binding stability toward gB.
Mangiferin / 3NWF (gB)	−7.3	ASN548, ALA561, CYS116	ARG599, ALA629	Stable binding with moderate inhibitory potential against gB.
Myricetin 5-methyl ether / 3NWF (gB)	−6.9	GLU619, SER560, ALA561, GLY618	ARG599, ALA629	Moderate affinity with favourable interaction stability.
Homomangiferin / 3NWF (gB)	−7.2	ASN548, SER560, CYS116	ARG599, ALA629	Formed stable ligand–protein interactions indicating promising antiviral activity.
Apigenin-7-glucuronide-4′-(6′′-malonylglucoside) / 3NWF (gB)	−8.5	ASN548, ASN546, GLU622, GLU619, ALA561, PRO119, GLY556	VAL563, ALA549	Strongest interaction with gB, suggesting excellent inhibitory potential and high complex stability.
Quercetin / 3NWF (gB)	−7.2	ASN548, ALA561, PRO119, SER560, THR626	ARG624, LEU536	Strong and stable binding interactions with favourable inhibitory characteristics.
Oroxylin A / 3NWF (gB)	−6.9	THR554	TRP539, VAL553, LEU356	Moderate binding affinity supported by hydrophobic stabilisation.
D-Gluconic acid / 4MYV (gD)	−5.4	SER140, ASP139, TYR164, SER142, PHE141, THR160	–	Weak binding affinity with comparatively low inhibitory effectiveness against gD.
Mangiferin / 4MYV (gD)	−7.8	SER140, ASP139, HIS154, TYR138	ILE197, LEU195	Moderate interaction strength and acceptable binding stability.
Myricetin 5-methyl ether / 4MYV (gD)	−8.5	ASP139, HIS154, ARG101	LEU195, ILE108, ILE110, ILE197	Strong binding affinity indicating excellent potential as a gD inhibitor.
Homomangiferin / 4MYV (gD)	−7.4	SER140, SER142	ALA157, LEU195, ILE197	Stable interactions and promising antiviral binding behavior.
Apigenin-7-glucuronide-4′-(6′′-malonylglucoside) / 4MYV (gD)	−9.4	ARG101, TYR104, SER142, HIS154, ASP139, TYR137, SER140, TRP135, LEU220	PHE141, LEU195	Highest binding affinity among all compounds, indicating exceptional inhibitory potential against gD.
Quercetin / 4MYV (gD)	−8.4	ALA155, SER142	ALA157, THR160, LEU195, TYR138, ILE110	Strong ligand–protein interactions with significant binding stability.
Oroxylin A / 4MYV (gD)	−7.7	SER142, PRO156	ALA157, LEU195, ILE110	Favourable binding interactions and potential antiviral activity against gD.

Two compounds that showed strong binding affinity towards gB are homomangiferin and Apigenin 7-glucuronide-4′-(6′′ malonyl-glucoside). Five compounds have strong binding towards gD, including mangiferin, myricetin 5-methyl ether, homomangiferin, apigenin 7-glucuronide-4'-(6'' malonylglucoside), and quercetin. Homomangiferin is the top lead binder to both gB and gD. In summary, the flavonols (myricetin and quercetin) may form more stable, long-term complexes with the viral entry proteins compared to the xanthone mangiferin. This evidence suggests that when HHV-1-infected cells are treated with the extract, a specific reaction occurs between gB and gD and the compounds from the flavonoid group. A high binding affinity is critical for disrupting viral survival and the subsequent production of new viral proteins.

Binding of compounds to Human Serum Albumin (HSA)

Docking simulations of HSA with selected antiviral compounds revealed varying binding affinities at two primary binding sites:

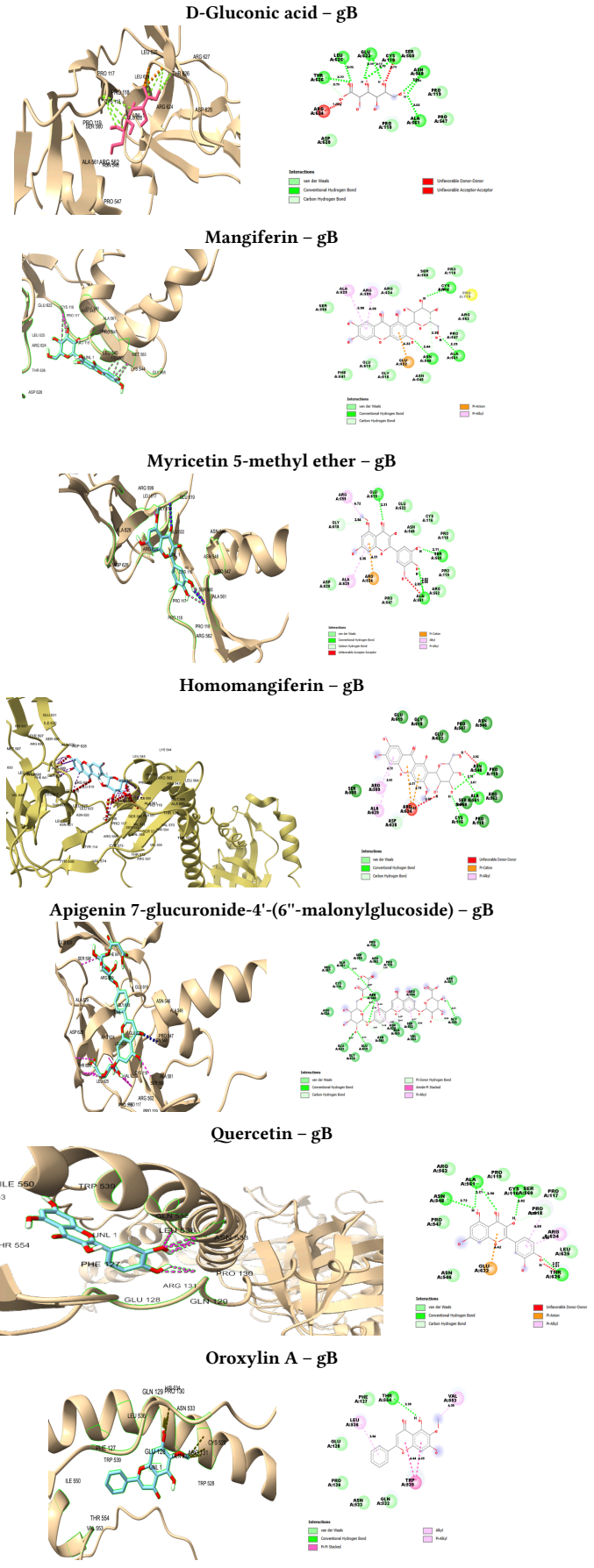

Fig. 3. (Left) Molecular docking of compounds as ligands to virus glycoprotein gB (3NWF). (Right) Interaction between amino acids of the respective glycoprotein and the compound. Green dotted lines indicate hydrogen bond interactions between amino acids and ligand. Pink dotted lines indicate Pi-Pi interactions between amino acids of gB (3NWF). Values adjacent to the dotted lines indicate interaction distances (Å).

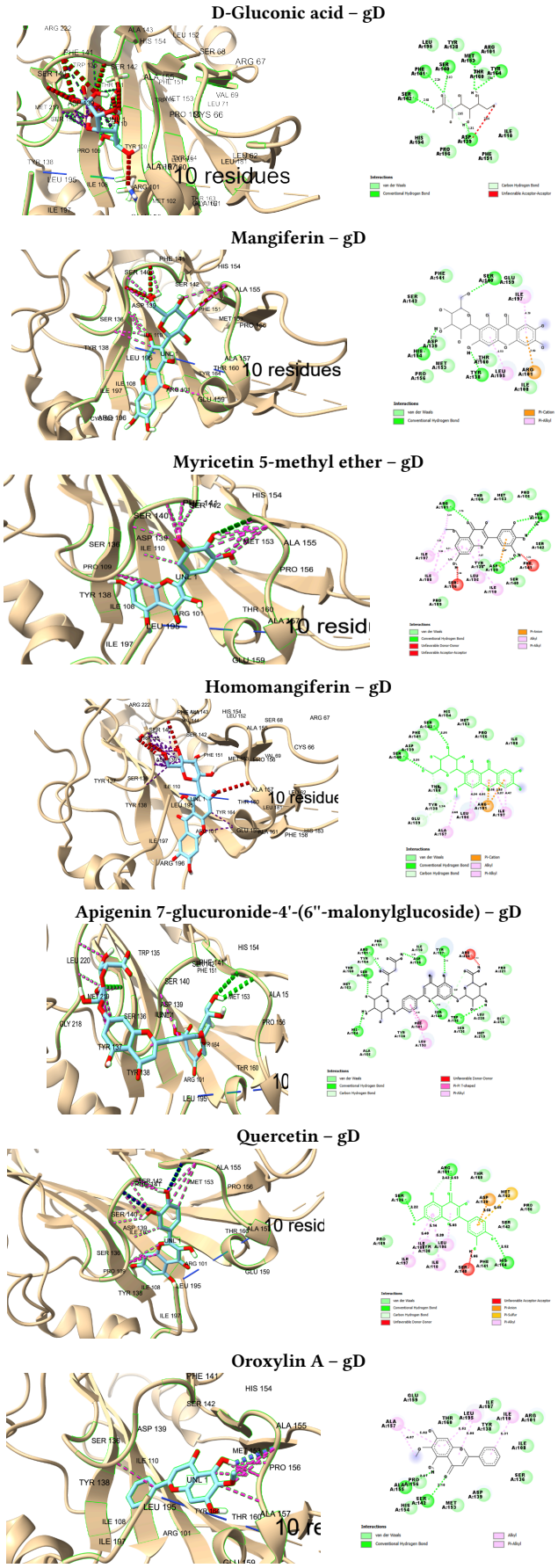

Fig. 4. (Left) Molecular docking of compounds as ligands to virus glycoprotein gD (4MYV). (Right) Interaction between amino acids of the respective glycoprotein and the compound. Green dotted lines indicate hydrogen bond interactions between amino acids and ligand. Pink dotted lines indicate Pi-Pi interactions between amino acids of gD (4MYV). Values adjacent to the dotted lines indicate interaction distances (Å).

site I (subdomain IIA) and site II (subdomain IIIA) (Table 8). Homomangiferin demonstrated the strongest binding affinity at site I with a mean binding energy of −12.39 kcal/mol, followed closely by mangiferin (-12.11 kcal/mol), as represented in Figure 5A(I) and 5B(I). The docking studies revealed that active compounds from PMFPAE demonstrate favourable binding affinities (Table 8), especially at site I of HSA (subdomain IIA). Binding energies below about −8 kcal/mol are often used as a practical cutoff for potentially active ligands in drug design (Ivanova & Karelson, 2022). Several intermolecular forces involved in the complexation of PMFPAE with human serum albumin are also illustrated in Figure 5A(II) and 5B(II). It is important to note that an unfavourable donor–donor interaction is also observed; however, this does not substantially compromise the overall stability due to the dominance of favourable interactions (Chen *et al.*, 2016).

DISCUSSION

The initial step of HHV-1 entry into cells is the binding of virion envelope gB and gC to cell surface receptors, preferably heparan sulfate (Jambunathan *et al.*, 2021). Viral entry involves virion envelope fusion with the host cell membrane and relies upon gD, heterodimer gH/gL, gB, and a gD receptor. High-affinity binding of gD to one or more of its cell surface receptors induces a conformational change that allows gB, gH and gL to be recruited as components of a fusion complex. The fusion complex results in the integration between the lipid bilayer and its contents, mixing with released viral tegument and nucleocapsid proteins, which all occur inside the host cytoplasm (Agelidis & Shukla, 2015). Binding of compounds from PMFPAE to gB and gD stops these initial steps, hampering viral entry into the host cells, as evidenced by this study, where the gene expression of UL27 was inhibited and the docking

Table 8. Mean binding energy of compounds to Sites I and II of Human Serum Albumin.

Compound	Mean binding energy Site I (kcal/mol)	Mean binding energy Site II (kcal/mol)
D-Gluconic acid	−5.02	−5.42
Mangiferin	−12.11	−8.38
Myricetin 5-methyl ether	−10.94	−8.38
Homomangiferin	−12.39	−7.79
Apigenin-7-glucuronide-4′-(6′‘-malonylglucoside)	−10.86	−8.23
Quercetin	−10.13	−7.58
Oroxylin A	−8.89	−6.79

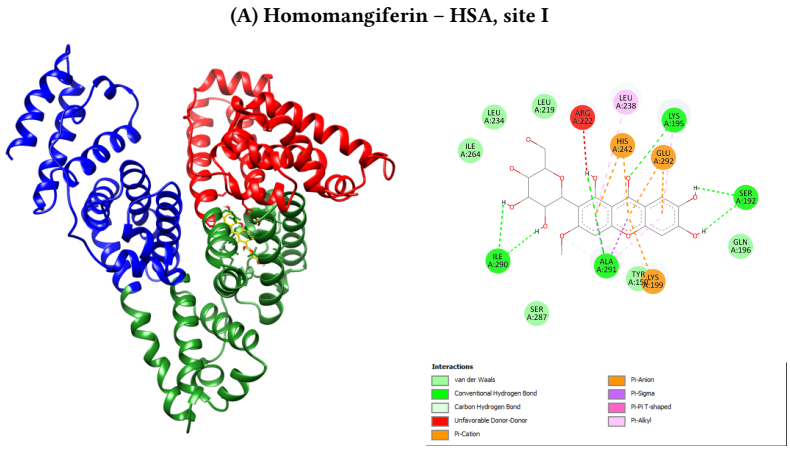

Fig. 5. (I) The binding orientation of the lowest docking energy conformation of compounds on the molecular surface representation of the docking, and (II) the intermolecular forces involved and the participating amino acid residues, of homomangiferin (A) and mangiferin (B) on HSA (PDB ID: 1BM0). HSA domains are colour-coded: domain I red, domain II green, domain III blue.

studies. This molecular suppression provides a mechanistic basis for the high plaque inhibition percentages observed in previous time-of-removal studies (Ismaeel *et al.*, 2022), confirming that PMFPAE's antiviral activity spans from early entry to the late-stage assembly and reinfection of viral progeny. Downregulation of *UL27* will reduce the expression of gB, the mandatory glycoprotein of the virus capsid that attaches to the host receptor during fusion (Cattaneo *et al.*, 2025). For further clarification on the effect on gB, a protein expression study will be needed, but in this study, we have proven the interaction with gB in an in silico study that will be explained below.

Virucidal activity of *Eleusine indica* has previously been shown and related to the down-regulation of UL27 transcription at 2 HPI, representing the immediate early phase of virus replication, and 8 HPI (early replication phase) (Iberahim *et al.*, 2018). Virucidal activity by PMFPAE has also been shown by Ismaeel *et al.* (2024) and has been indicated by other researchers, as stated in Table 2, in particular provided by mangiferin. Mangiferin is a major constituent of *P. macrocarpa*. It significantly reduces the expression of immediate-early and early (E) genes, such as UL54 and UL42 (Wang & Chen, 2023). Because viral gene expression occurs in a tightly regulated cascade, the inhibition of these earlier genes naturally leads to a downregulation of late genes such as UL27 (Ma *et al.*, 2016; Wang & Chen, 2023). Mangiferin has been previously determined to be beneficial pharmacologically in treating herpesvirus-related diseases (Rechenchoski *et al.*, 2020).

Similarly, quercetin and its derivatives (e.g., isoquercitrin) block the expression of IE proteins (like ICP27), which are required to trigger the transcription of the UL27 gene (Kim *et al.*, 2020; Kim *et al.*, 2021). Quercetin antiviral activities have been attributed to multiple mechanisms, including direct virucidal effects, inhibition of viral replication cycles, and modulation of host immune responses (Petrillo *et al.*, 2021). In addition, quercetin may provide anti-inflammatory activity in several ways, as discussed by Ruiz *et al.* (2007) and Martínez-Flórez *et al.* (2005). In essence, quercetin can also act as an immunomodulator by reducing cellular distress signals and chemotactic factors. It tempers the recruitment of hyper-aggressive immune cells to the delicate site of infection without completely turning off the host's ability to clear the virus.

Apigenin is another compound discovered in PMFPAE. It is a tiny flavone-derived molecule that serves as the aglycone of different natural element glycosides (Qiu *et al.*, 2019). The synergistic role of flavonoids such as apigenin has shown that it can interfere with late events in the viral replication cycle and reduce the production of viral progeny (Rittà *et al.*, 2020). It specifically inhibits the lytic cycle and has been associated with reduced cell-to-cell spread, a function primarily mediated by the UL27-encoded glycoprotein B (Wu *et al.*, 2017; Rittà *et al.*, 2020). Apigenin was found capable of causing cell cycle arrest, limiting cell migration and invasion, generating an immune response, and triggering cell apoptosis and autophagy (Salehi *et al.*, 2019). Consequently, HHV-1 fails to replicate in the cells.

Myricetin and Oroxylin A are also flavonoids that contribute to the extract's overall antiviral profile by deactivating host pathways (like NF-κB) that the virus requires for efficient gene expression across all phases, as previously reported by Hu *et al.* (2022) and Ma *et al.* (2016). Through direct contact with the viral gD protein, myricetin has been shown to block HHV infection by interfering with virus adsorption and membrane fusion (Li *et al.*, 2020).

D-gluconic acid is a polysaccharide-rich fraction of PMFPAE. It inhibits viral replication by inhibiting virus attachment or penetration (Santoyo *et al.*, 2012). D-gluconic acid from *Dunaliella salina* and *Haematococcus pluvialis* extracts has been shown to affect viral replication by inhibiting virus attachment or penetration.

In this study, Homomangiferin emerges as the premier lead candidate, achieving a remarkable binding affinity and superior performance, which is attributed to its complex xanthone scaffold, which facilitates deep penetration into the gD binding pocket and establishes a robust network of hydrogen bonds and electrostatic interactions with key residues such as TRP135 and TYR137. By effectively anchoring within this site, Homomangiferin demonstrates the strongest potential to prevent the conformational changes necessary for viral-host membrane fusion, potentially neutralising HHV-1 entry. Because of this strong complementarity, homomangiferin shows the highest potential to disrupt the HHV-1 viral entry process, as observed in Ismaeel *et al.* (2024), by effectively "blocking" the gB. Homomangiferin also disrupts HHV-1 by interacting with the gD entry process, effectively "blocking" the gB glycoprotein, as explained by Fan *et al.* (2015).

All of the compounds found in PMFPAE play a significant role in contributing to the multifaceted antiviral activity. Bioactive compounds with anti-inflammatory and antioxidant activities (Andrean *et al.*, 2014; Lee & Park, 2016), such as Oroxylin A and homomangiferin, were also present in PMFPAE. Herpes virus 1 has been reported to induce brain inflammation and multifocal demyelination in rats' brains (Boukhvalova *et al.*, 2019). Having a compound with anti-inflammatory activity may be important in counteracting this activity during HHV-1 infection. In addition, the antioxidant property of homomangiferin, a xanthone derivative, directly neutralizes highly reactive superoxides, hydroxyl radicals, and hydrogen peroxides generated during viral replication before they can inflict damage (Khurana *et al.*, 2016).

HSA plays a crucial role in the pharmacokinetics of antiviral compounds, significantly influencing drug distribution and metabolism within the bloodstream (Tayyab & Feroz, 2021). Homomangiferin displayed the highest binding energy, though hindered by an unfavourable donor-donor interaction with Arg-222. Meanwhile, mangiferin, with a slightly lower binding energy of −12.11 kcal/mol, showed a broader range of favourable interactions, especially through van der Waals and π-interactions. These docking results shed light on the potential interactions of these antiviral compounds with HSA, particularly at the primary drug-binding sites. The strong binding affinities observed, especially for mangiferin and homomangiferin at site I, suggest that these compounds may be effectively transported in the bloodstream, enhancing their stability and half-life. This site is also a known binding region for antiviral drugs, such as acyclovir, which are commonly used in the treatment of herpes virus infections (Abdelhameed *et al.*, 2017). HSA can act as a valuable transporter, reducing drug leakage and extending drug stability during systemic circulation while protecting against enzymatic degradation (Li *et al.*, 2023). Furthermore, HSA itself has an estimated circulation half-life of about 19 days, further aiding in prolonging the half-life of administered drugs. This study highlights the significance of protein-ligand interactions in optimising the design of antiviral drugs, with the potential to improve their therapeutic efficacy against viral infections.

The potent anti-HHV-1 activity demonstrated by PMFPAE cannot be attributed to a single isolated constituent, but rather to the synergistic interplay among its diverse phytochemical groups. Co-existence of organic acids, xanthones, and multiple flavonoids, as shown by LC-MS/MS and confirmed by the in silico molecular docking and previous reports (Ismaeel *et al.*, 2022; Ismaeel *et al.*, 2024), supports this view. Although this study has shown the potential of PMFPAE in anti-HHV-1 activity posed by the bioactive compounds, it is recommended that future studies be done to validate the in

silico mechanistic effects in in vivo settings for antiviral efficacy studies in animal models, thorough pharmacodynamic studies, and, importantly, formulation development, as the compounds available may need to be standardised.

CONCLUSION

PMFPAE contains a combination of seven main compounds that enhance its effectiveness against HHV-1 and also display antioxidant and anti-inflammatory activities. Expression of the UL27 gene during HHV-1 replication is suppressed by PMFPAE, in particular during the late replication phase, which may affect the gB from forming and functioning in virus attachment. The main antiviral mechanism, as shown by the in silico study, is the binding of compounds to virus surface glycoproteins gB and gD, in particular homomangiferin. Almost all the compounds have drug-likeness properties, as shown by the SwissADME analysis, with quercetin, mangiferin, and myricetin 5-methyl ether showing the fewest rule violations. Toxicity ProTox-II prediction classified D-gluconic acid as non-toxic; myricetin 5-methyl ether, Oroxylin A, and the Apigenin derivative were the least toxic, with homomangiferin exhibiting manageable toxicity but standing out as a viable lead. Quercetin and Mangiferin both exhibited the highest toxicity. From a pharmacological perspective, Homomangiferin and the Apigenin derivative are the strongest candidates to be considered as drugs because they combine high safety profiles with exceptional binding affinities against viral proteins. Ensemble learning models confirmed all seven ligands are non-carcinogens. PMFPAE is more suitable as a supplement or topical agent due to the low GI absorption and specific toxicity profiles of some compounds. However, specific leads like homomangiferin still hold potential for future anti-herpetic agents once safety is validated in vivo. By targeting specific viral genes and proteins, PMFPAE effectively disrupts viral replication during its various phases.

ACKNOWLEDGEMENTS

The authors express their gratitude to the Malaysian Ministry of Higher Education for their partial funding of our research (FRGS/1/2019/WAB11/UKM/02/1).

ETHICAL STATEMENT

Not applicable.

CONFLICT OF INTEREST

The authors declare no conflict of interest.

REFERENCES

Abdelhameed, A.S., Bakheit, A.H., Almutairi, F.M., AlRabiah, H. & Kadi, A.A. 2017. Biophysical and in silico studies of the interaction between the anti-viral agents acyclovir and penciclovir, and human serum albumin. Molecules, 22(11): 1906. https://doi.org/10.3390/molecules22111906

Agelidis, A.M. & Shukla, D. 2015. Cell entry mechanisms of HSV: What we have learned in recent years. Future Virology, 10(10): 1145-1154. https://doi.org/10.2217/fvl.15.85

Andrean, D., Prasetyo, S., Kristijarti, A. P., & Hudaya, T. 2014. The extraction and activity test of bioactive compounds in *Phaleria macrocarpa* as antioxidants. Procedia Chemistry, 9: 94–101. https://doi.org/10.1016/j.proche.2014.05.012

Azher, T., Yin, X.-T., Tajfirouz, D., Huang, A., & Stuart, P. M. 2017. Herpes simplex keratitis: challenges in diagnosis and clinical management. Clinical Ophthalmology, 11: 185–191. https://doi.org/10.2147/opth.s80475

Bakar, K.A., Lam, S.D. & Feroz, S.R. 2024. Binding characteristics of the major kratom alkaloid, mitragynine, towards serum albumin: Spectroscopic, calorimetric, microscopic, and computational investigations. Chemico-Biological Interactions, 404: 111264. https://doi.org/10.1016/j.cbi.2024.111264

Banerjee, P., Eckert AO, Schrey AK, Preissner R. 2018. ProTox-II: A webserver for the prediction of toxicity of chemicals. Nucleic Acids Research, 46(W1): W257–W263. https://doi.org/10.1093/nar/gky318

Biancatelli, R.M.L.C., Berrill, M., Catravas, J.D. & Marik, P.E. 2020. Quercetin and vitamin C: An experimental, synergistic therapy for the prevention and treatment of SARS-CoV-2 related disease (COVID-19). Frontiers in Immunology, 11: 1451. https://doi.org/10.3389/fimmu.2020.01451

Bin, L., Edwards, M.G., Heiser, R.A., Streib, J.E., Richers, B., Hall, C.F. & Leung, D.Y.M. 2014. Identification of novel gene signatures in patients with atopic dermatitis complicated by eczema herpeticum. Journal of Allergy and Clinical Immunology, 134(4): 848–855. https://doi.org/10.1016/j.jaci.2014.07.018

Boukhvalova, M. S., Mortensen, E., Mbaye, A., Lopez, D., Kastrukoff, L. & Blanco, J. C. 2019. Herpes simplex virus 1 induces brain inflammation and multifocal demyelination in the cotton rat *Sigmodon hispidus*. Journal of Virology, 94(1): e01161-19. https://doi.org/10.1128/jvi.01161-19

Cattaneo, S., Bettegazzi, B., Ingusci, S., Gianluca Verlengia, G., Tascini, A.S., Zucchini, S., Codazzi, F., Morelli, M.J., Marzulli, M., Glorioso, J.C. & Simonato, M. 2025. Genetic mutations in HSV-1 replication-defective vectors: Implications for their safety in gene therapy applications. Gene Therapy, 32: 581–593. https://doi.org/10.1038/s41434-025-00566-1

Chen, D., Oezguen, N., Urvil, P., Ferguson, C., Dann, S.M. & Savidge, T.C. 2016. Regulation of protein-ligand binding affinity by hydrogen bond pairing. Science Advances, 2(3): e1501240. https://doi.org/10.1126/sciadv.1501240

Chiang, L.C., Chiang, W., Liu, M.C. & Lin, C.C. 2003. In vitro antiviral activities of *Caesalpinia pulcherrima* and its related flavonoids. Journal of Antimicrobial Chemotherapy, 52(2): 194–198. https://doi.org/10.1093/jac/dkg291

Crimi, S., Fiorillo, L., Bianchi, A., D'Amico, C., Amoroso, G., Gorassini, F., Mastroieni, R., Marino, S., Scoglio, C., Catalano, F., Campagna, P., Bocchieri, S., Stefano, R. D., Fiorillo, M. T., & Cicciù, M. 2019. Herpes Virus, Oral Clinical Signs and QoL: Systematic Review of Recent Data. Viruses, 11(5): 463. https://doi.org/10.3390/v11050463

Dähne, T., Jaki, L., Gosert, R., Fuchs, J., Krumbholz, A., Nägele, K., Pletz, M.W., Khanna, N., Leuzinger, K. & Panning, M. 2025. Herpes simplex virus and drug resistance—comprehensive update on resistance mutations and implications for clinical management: a narrative review. Clinical Microbiology and Infection, 31: 1484-1490. https://doi.org/10.1016/j.cmi.2025.04.046

Daina, A., Michielin, O., & Zoete, V. 2017. SwissADME: a free web tool to evaluate pharmacokinetics, drug-likeness and medicinal chemistry friendliness of small molecules. Scientific Reports, 7: 42717. https://doi.org/10.1038/srep42717

Du, S., Liu, H., Lei, T., Xie, X., Wang, H., He, X., Tong, R., & Wang, Y. 2018. Mangiferin: An effective therapeutic agent against several disorders. Molecular Medicine Reports, 18: 4775-4786. https://doi.org/10.3892/mmr.2018.9529

Ezike, T.C., Okpala, U.S., Onoja, U.L., Nwike, C.P., Ezeako, E.C., Okpara, O.J., Okoroafor, CC., Eze, S.C., Kalu, O.L., Odoh, E.C., Nwadike, U.G., Ogbodo, J.O., Umeh, B.U., Ossai, E.C., & Nwanguma, B.C. 2023. Advances in drug delivery systems, challenges and future directions. Heliyon, 9(6): e17488. https://doi.org/10.1016/j.heliyon.2023.e17488

Fan, Q., Longnecker, R. & Connolly, S.A. 2015. A functional interaction between herpes simplex virus 1 glycoprotein gH/gL domains I and II and gD is defined by using Alphaherpesvirus gH and gL chimeras. Journal of Virology, 89(14): 7159-7169. https://doi.org/10.1128/jvi.00740-15

Farooq, A. V., & Shukla, D. 2012. Herpes Simplex Epithelial and Stromal Keratitis: An Epidemiologic Update. Survey of Ophthalmology, 57(5): 448–462. https://doi.org/10.1016/j.survophthal.2012.01.005

Gnann, J. W., Barton, N., & Whitley, R. J. 1983. Acyclovir: Mechanism of action, pharmacokinetics, safety and clinical applications. Pharmacotherapy: The Journal of Human Pharmacology and Drug Therapy, 3(5): 275–283. https://doi.org/10.1002/j.1875-9114.1983.tb03274.x

Hernández-Santoyo, A., Tenorio-Barajas, A. Y., VictorAltuzar, Vivanco-Cid, H., & Mendoza-Barrera, C. 2013. Protein-protein and protein-ligand docking. In: Contact-less assessment of in-vivo body signals using microwave doppler radar. Intech, Slovakia. https://doi.org/10.5772/56376

Horai, H., Arita, M., Kanaya, S., Nihei, Y., Ikeda, T., Suwa, K., Ojima, Y., Tanaka, K., Tanaka, S., Aoshima, K., Oda, Y., Kakazu, Y., Kusano, M., Tohge, T., Matsuda, F., Sawada, Y., Hirai, M. Y., Nakanishi, H., Ikeda, K. & Nishioka, T. 2010. MassBank: a public repository for sharing mass spectral data for life sciences. Journal of Mass Spectrometry, 45(7): 703–714. https://doi.org/10.1002/jms.1777

Hu, H., Hu, Z., Zhang, Y., Wan, H., Yin, Z., Li, L., Liang, X., Zhao, X., Yin, L., Ye, G., Zou, Y., Tang, H., Jia, R., Chen, Y., Zhou, H., & Song, X. 2022. Myricetin inhibits pseudorabies virus infection through direct inactivation and activating host antiviral defense. Frontiers in Microbiology, 13: 985108. https://doi.org/10.3389/fmicb.2022.985108

Hua, Y., & Jenke, D. 2012. Increasing the Sensitivity of an LC-MS Method for Screening Material Extracts for Organic Extractables via Mobile Phase Optimization. Journal of Chromatographic Science, 50(3): 213–227. https://doi.org/10.1093/chromsci/bmr049

Huey, R., & Morris, G. M. 2008. Using AutoDock 4 with AutoDocktools: a tutorial. The Scripps Research Institute Molecular Graphics Laboratory, California, USA.

Iberahim, R., Nor, N. S. M., Yaacob, W. A., & Ibrahim, N. 2018. *Eleusine indica* Inhibits Early and Late Phases of Herpes Simplex Virus Type 1 Replication Cycle and Reduces Progeny Infectivity. Sains Malaysiana, 47(7): 1431–1438. https://doi.org/10.17576/jsm-2018-4707-10

Ismaeel, M. Y. Y., Dyari, H. R. E., & Ibrahim, N. 2022. Protein from *Phaleria macrocarpa* Fruit Aqueous Extract Inhibits Early and Late Replication Phases of Human Herpes Virus Type-1. Pharmacognosy Journal, 14(1): 39–45. https://doi.org/10.5530/pj.2022.14.6

Ismaeel, M., Dyari, H. R. E., Nor, N. S. M., Yaacob, W. A., & Ibrahim, N. 2018a. Anti-human herpesvirus type-1 activity of *Phaleria macrocarpa* fruits methanol extract and fractions. Malaysian Applied Biology, 47(5): 31–40.

Ismaeel, M. Y. Y., Dyari, H. R. E., Yaacob, W. A., & Ibrahim, N. 2018b. In vitro antiviral activity of aqueous extract of *Phaleria macrocarpa* fruit against herpes simplex virus type 1. AIP Conference Proceedings, 1940: 020076. https://doi.org/10.1063/1.5027991

Ismaeel, M. Y. Y., Yaacob, W. A., Tahir, M. M., & Ibrahim, N. 2015. Phytochemical screening, cytotoxicity and antiviral activity of hexane fraction of *Phaleria macrocarpa* fruits. AIP Conference Proceedings, 1678: 030012. https://doi.org/10.1063/1.4931233

Ismaeel, M. Y. Y., Yip, C. W., Nor, N. S. M., & Ibrahim, N. 2024. *Phaleria macrocarpa* fruit protein aqueous extract affects viral entry, virucidal activity, and progeny release. Malaysian Applied Biology, 53(4): 77–87. https://doi.org/10.55230/mabjournal.v53i4.3095

Ivanova, L. & Karelson, M. 2022. The Impact of software used and the type of target protein on molecular docking accuracy. Molecules, 27(24): 9041. https://doi.org/10.3390/molecules27249041

Jambunathan, N., Clark, C.M., Musarrat, F., Chouljenko, V.N., Rudd, J. & Kousoulas, K.G. 2021. Two sides to every story: Herpes simplex type-1 viral glycoproteins gB, gD, gH/gL, gK, and cellular receptors function as key players in membrane fusion. Viruses, 13: 1849. https://doi.org/10.3390/v13091849

Kalusalingam, A., Kamal, K., Khan, A., Menon, B., Tan, C. S., Narayanan, V., Kumar, S., Goh, K. W., Lee, K. S., Chew, J., & Ming, L. C. 2024. *Phaleria macrocarpa* (Scheff.) Boerl. in ethnopharmacology: Pharmacognosy, safety, and drug development perspectives. Progress In Microbes & Molecular Biology, 7(1): a0000452. https://doi.org/10.36877/pmmb.a0000452

Khurana, R. K., Kaur, R., Lohan, S., Singh, K. K., & Singh, B. 2016. Mangiferin: a promising anticancer bioactive. Pharmaceutical Patent Analyst, 5(3): 169–181. https://doi.org/10.4155/ppa-2016-0003

Kim, B., Kim, Y.S., Hwang, Y., Yang, H.J., Li, W., Kwon, E., Kim, T.I., Go, Y. & Choi, J. 2021. *Quercus acuta* Thunb. (Fagaceae) and its component, isoquercitrin, inhibit HSV-1 replication by suppressing virus-induced ROS production and NF-κB activation. Antioxidants, 10(10): 1638. https://doi.org/10.3390/antiox10101638

Kim, C.H., Kim, J. & Song, Y. 2020. Antiviral activities of quercetin and isoquercitrin against human herpesviruses. Molecules, 25(10): 2379. https://doi.org/10.3390/molecules25102379

Kim, S.K., Shakya, A.K., & O'Callaghan, D.J. 2016. Full trans-activation mediated by the immediate-early protein of equine herpesvirus 1 requires a consensus TATA box, but not its cognate binding sequence. Virus Research, 211: 222–232. https://doi.org/10.1016/j.virusres.2015.10.026

Kovačević, S.Z., Jevrić, L.R., Podunavac Kuzmanović, S.O. & Lončar, E.S. 2014. Prediction of in-silico ADME properties of 1,2-O-isopropylidene aldohexose derivatives. Iranian Journal of Pharmaceutical Research, 13(3): 899-907.

Laine, R.F., Albecka, A., Linde, S-vd, Rees, E.J., Crump, C.M. & Kaminski, C.F. 2015. Structural analysis of herpes simplex virus by optical super-resolution imaging. Nature Communications, 6(1): 5980. https://doi.org/10.1038/ncomms6980

Lay, M.M., Karsani, S.A., Mohajer, S. & Malek, S.N.A. 2014. Phytochemical constituents, nutritional values, phenolics, flavonols, flavonoids, antioxidant and cytotoxicity studies on *Phaleria macrocarpa* (Scheff.) Boerl fruits. BMC Complementary and Alternative Medicine, 14(1): 152. https://doi.org/10.1186/1472-6882-14-152

Lee, J.Y. & Park, W. 2016. Anti-inflammatory effects of oroxylin A on RAW 264.7 mouse macrophages induced with polyinosinic-polycytidylic acid. Experimental and Therapeutic Medicine, 12(1): 151–156. https://doi.org/10.3892/etm.2016.3320

Lee, S., Lee, H. H., Shin, Y. S., Kang, H. & Cho, H. 2017. The anti-HSV-1 effect of quercetin is dependent on the suppression of TLR-3 in Raw 264.7 cells. Archives of Pharmacal Research, 40(5): 623–630. https://doi.org/10.1007/s12272-017-0898-x

Li, C., Zhang, D., Pan, Y.-J., & Chen, B. 2023. Human serum albumin based nanodrug delivery systems: Recent advances and future perspective. Polymers, 15(16): 3354. https://doi.org/10.3390/polym15163354

Li, W., Xu, C., Cui, H., Zhang, Y., Wang, Z., Wang, S., & Wang, W. 2020. Inhibition of herpes simplex virus by myricetin through targeting viral gD protein and cellular EGFR/PI3K/Akt pathway. Antiviral Research, 177: 104714. https://doi.org/10.1016/j.antiviral.2020.104714

Lipinski, C.A., Lombardo, F., Dominy, B.W. & Feeney, P.J. 2001. Experimental and computational approaches to estimate solubility and permeability in drug discovery and development settings. Advanced Drug Delivery Reviews, 46(1-3): 3-26. https://doi.org/10.1016/S0169-409X(00)00129-0

Livak, K.J. & Schmittgen, T.D. 2001. Analysis of relative gene expression data using real-time quantitative PCR and the 2−ΔΔCT method. Methods, 25(4): 402–408. https://doi.org/10.1006/meth.2001.1262

Ma, F., Shen, W.-W., Zhang, X., Li, M., Wang, Y., Zou, Y., Li, Y.-L., & Wang, H. 2016. Anti-HSV activity of kuwanon X from mulberry leaves with genes expression inhibitory and HSV-1 induced NF-κB deactivated properties. Biological and Pharmaceutical Bulletin, 39(10): 1667–1674. https://doi.org/10.1248/bpb.b16-00401

Martínez-Flórez, S., Gutiérrez-Fernández, B., Sánchez-Campos, S., González-Gallego, J. & Tuñón, M.J. 2005. Quercetin attenuates nuclear factor-kappaB activation and nitric oxide production in interleukin-1 beta-activated rat hepatocytes. Journal of Nutrition, 135(6): 1359–1365. https://doi.org/10.1093/jn/135.6.1359

Masibo, M., & He, Q. 2008. Major mango polyphenols and their potential significance to human health. Comprehensive Reviews in Food Science and Food Safety, 7(4): 309–319. https://doi.org/10.1111/j.1541-4337.2008.00047.x

Pattanaik, S. S., & Bhadra, P. 2020. In silico analysis of hepatoprotective properties of bael leaves. Indian Journal of Natural Sciences, 10(60): 20755-20757.

Petrillo, A. D., Orrù, G., Fais, A., & Fantini, M. C. 2021. Quercetin and its derivates as antiviral potentials: A comprehensive review. Phytotherapy Research, 36(1): 266–278. https://doi.org/10.1002/ptr.7309

Piret, J., & Boivin, G. 2011. Resistance of herpes simplex viruses to nucleoside analogues: mechanisms, prevalence, and management. Antimicrobial Agents and Chemotherapy, 55(2): 459-472. https://doi.org/10.1128/aac.00615-10

Qiu, J.-G., Wang, L., Liu, W., Wang, J., Zhao, E., Zhou, F.-M., Ji, X.-B., Wang, L., Xia, Z.-K., Wang, W., Lin, M.C.-M., Liu, L.-Z., Huang, Y.-X. & Jiang, B.-H. 2019. Apigenin Inhibits IL-6 transcription and suppresses esophageal carcinogenesis. Frontiers in Pharmacology, 10: 1002. https://doi.org/10.3389/fphar.2019.01002

Rechenchoski, D.Z., Agostinho, K.F., Faccin-Galhardi, L.C., Lonni, A.A.S.G., da Silva, J.V.H., de Andrade, F.G., Cunha A.P., Ricardo, N.M.P.S., Nozawa, C. & Linhares, R.E.C. 2020. Mangiferin: A promising natural xanthone from *Mangifera indica* for the control of acyclovir–resistant herpes simplex virus 1 infection. Bioorganic & Medicinal Chemistry, 28(5): 115304. https://doi.org/10.1016/j.bmc.2020.115304

Rittà, M., Marengo, A., Civra, A., Lembo, D., Cagliero, C., Kant, K., Lal, U. R., Rubiolo, P., Ghosh, M., & Donalisio, M. 2020. Antiviral activity of a *Arisaema tortuosum* leaf extract and some of its constituents against herpes simplex virus Type 2. Planta Medica, 86(4): 267–275. https://doi.org/10.1055/a-1087-8303

Ruiz, P.A., Braune, A., Hölzlwimmer, G., Quintanilla-Fend, L. & Haller D. 2007. Quercetin inhibits TNF-induced NF-kappaB transcription factor recruitment to proinflammatory gene promoters in murine intestinal epithelial cells. Journal of Nutrition, 137(5): 1208–1215. https://doi.org/10.1093/jn/137.5.1208

Saakre, M., Mathew, D. & Ravisankar, V. 2021. Perspectives on plant flavonoid quercetin-based drugs for novel ARS-CoV-2. Beni-Suef University Journal of Basic and Applied Sciences, 10: 21. https://doi.org/10.1186/s43088-021-00107-w

Salehi, B., Venditti, A., Sharifi-Rad, M., Kręgiel, D., Sharifi-Rad, J., Durazzo, A., Lucarini, M., Santini, A., Souto, E. B., Novellino, E., Antolak, H., Azzini, E., Setzer, W.N., & Martins, N. 2019. The therapeutic potential of apigenin. International Journal of Molecular Sciences, 20(6): 1305. https://doi.org/10.3390/ijms20061305

Santoyo, S., Jaime, L., Plaza, M., Herrero, M., Rodriguez-Meizoso, I., Ibañez, E. & Reglero, G. 2012. Antiviral compounds obtained from microalgae commonly used as carotenoid sources. Journal of Applied Phycology, 24: 731-741. https://doi.org/10.1007/s10811-011-9692-1

Stampfer, S.D., Lou, H., Cohen, G.H., Eisenberg, R.J., Heldwein, E.E. 2010. Structural basis of local, pH-dependent conformational changes in glycoprotein B from herpes simplex virus type 1. Journal of Virology, 84(24): 12924-12933. https://doi.org/10.1128/JVI.01750-10

Tayyab, S., & Feroz, S. R. 2021. Serum albumin: clinical significance of drug binding and development as drug delivery vehicle. In: Advances in Protein

Chemistry and Structural Biology. Vol. 123. Academic Press. pp. 193–218. https://doi.org/10.1016/bs.apcsb.2020.08.003

Veber, D.F., Johnson, S.R., Cheng, H.Y., Smith, B.R., Ward, K.W., Kopple, K.D. 2002. Molecular properties that influence the oral bioavailability of drug candidates. Journal of Medicinal Chemistry, 45(12): 2615-2623. https://doi.org/10.1021/jm020017n

Wan, S., Bhati, A.P., Zasada, S.J., & Coveney, P.V. 2020. Rapid, accurate, precise and reproducible ligand–protein binding free energy prediction. Interface Focus, 10(6): 20200007. https://doi.org/10.1098/rsfs.2020.0007

Wang, W., & Chen, G. 2023. Antiviral activity of mangiferin from the rhizome of *Anemarrhena asphodeloides* against herpes simplex virus type 1. Asian Pacific Journal of Tropical Biomedicine, 13(3): 112–120. https://doi.org/10.4103/2221-1691.372284

Wang, Y., Wang, Q., Zhu, Q., Zhou, R., Liu, J., & Peng, T. 2011. Identification and characterization of acyclovir-resistant clinical HSV-1 isolates from children. Journal of Clinical Virology, 52(2): 107–112. https://doi.org/10.1016/j.jcv.2011.06.009

Wu, C.-C., Fang, C., Cheng, Y.-J., Hsu, H., Chou, S., Huang, S., Tsai, C.-H., & Chen, J. 2017. Inhibition of Epstein-Barr virus reactivation by the flavonoid apigenin. Journal of Biomedical Science, 24(1): 2. https://doi.org/10.1186/s12929-016-0313-9